

Design, Construction, and Installation of In-Glovebox Pumped Actinide Molten Salt Loops

Chemical and Fuel Cycle Technologies Division

About Argonne National Laboratory

Argonne is a U.S. Department of Energy laboratory managed by UChicago Argonne, LLC under contract DE-AC02-06CH11357. The Laboratory's main facility is outside Chicago, at 9700 South Cass Avenue, Argonne, Illinois 60439. For information about Argonne and its pioneering science and technology programs, see www.anl.gov.

Disclaimer

This report was prepared as an account of work sponsored by an agency of the United States Government. Neither the United States Government nor any agency thereof, nor UChicago Argonne, LLC, nor any of their employees or officers, makes any warranty, express or implied, or assumes any legal liability or responsibility for the accuracy, completeness, or usefulness of any information, apparatus, product, or process disclosed, or represents that its use would not infringe privately owned rights. Reference herein to any specific commercial product, process, or service by trade name, trademark, manufacturer, or otherwise, does not necessarily constitute or imply its endorsement, recommendation, or favoring by the United States Government or any agency thereof. The views and opinions of document authors expressed herein do not necessarily state or reflect those of the United States Government or any agency thereof, Argonne National Laboratory, or UChicago Argonne, LLC.

Design, Construction, and Installation of In-Glovebox Pumped Actinide Molten Salt Loops

prepared by
Nora A. Shaheen
Amber Polke
Denis J. Johnson
Nathaniel C. Hoyt
Chemical and Fuel Cycle Technologies Division, Argonne National Laboratory

September 30, 2025

Abstract

This report summarizes the work conducted in FY25 to construct and install pumped actinide-bearing molten salt loops in a radiological glovebox. The establishment of such a capability will provide a platform in which technologies developed for Gen. IV molten salt reactors may be tested under relevant operating conditions. A review of convective molten salt systems is provided to frame Argonne's pumped actinide loop relative to contemporary and historical systems. Moreover, the infrastructure needed to operate the system is detailed to provide additional context as to design metrics of the loops and supporting equipment. The pumps' performance in water testing is outlined and used to inform operational activities planned in FY26. Finally, electrochemical experiments investigating fundamental reaction mechanisms governing reactive oxygen species that promote corrosion of molten salt media is also reported. In total, these combined loop installation and sensor development tasks will serve to aid in the future commercial deployment of molten salt reactors in the U.S.

Acknowledgements

This report satisfies milestones M3AT-25AN0702031 (*Installation of Molten Salt Flow Loop with Chemistry Monitoring and Control System*) and M4AT-25AN0702032 (*Molten Salt Sensor Operations*) conducted under the U.S. Department of Energy's Molten Salt Reactor Campaign. Dr. Patricia Paviet is the National Technical Director and Janelle Eddins is the Federal Program Manager. The authors would like to acknowledge Jeff Trosen and Tyler Anderson for providing machining support, Dr. Drace Penley for supporting assembly efforts, and Guosheng Ye for conducting heat transfer simulations. This work was conducted at Argonne National Laboratory and supported by the U.S. Department of Energy, Office of Nuclear Energy, under Contract DE-AC02-06CH11357.

1. Introduction

A wide variety of molten salt reactor (MSR) designs and chemistries are currently under development for applications in Gen. IV nuclear reactors. The taxonomy of MSRs spans a range of neutron spectra (fast vs. thermal), molten salt chemistries (chloride- vs. fluoride-based salts), classes (e.g. homogeneous vs. heterogeneous), reactor families (e.g. graphite moderated MSR vs. heterogeneous chloride fast MSR), and MSR types (e.g. Pu-containing fluoride fast reactor vs. salt cooled reactor with fixed fuel). Domestic and international licensing requirements largely dictate taxonomy-independent regulatory frameworks. ^{2,3}

To enable commercial deployment of these reactors, the development of process monitoring technologies capable of withstanding long-term operation in MSRs is needed. However, only a limited number of these tools are at a sufficiently high technology readiness level (TRL) to facilitate commercial deployment.⁴ Moreover, testing of these technologies in practical conditions, wherein forced convection and non-isothermal environments prevail, has been limited. As such, modular platforms enabling rapid testing of under-development technologies are needed to evaluate the applicability of process monitoring technologies in a range of MSR taxonomies. Towards that end, the work presented herein describes the development of pumped, non-isothermal, actinide-bearing molten salt loops designed and constructed as a testing platform for equipment under relevant MSR conditions. To further contextualize this work, a historical and contemporary survey of existing molten salt flow loops and systems is provided. Additionally, the infrastructure required to meet the needs for such a testing platform is discussed.

Alongside work developing the actinide loop, Argonne also continued development of electrochemical sensors to support monitoring and control of molten salt flow systems. Electrochemical sensors are considered to be of sufficiently high TRL for applications in molten salt environments containing the actinide and lanthanide species encountered in MSRs. These sensors are capable of supporting material control and accountancy (MC&A) objectives as well as serving as an in-line process monitoring tool.^{5–8} Herein, we discuss the use of these sensors for the characterization of dissolved reactive oxygen species (ROSs, e.g. O²⁻, O₂²⁻, etc.). Understanding and quantifying these species is a critical step towards mitigating MC&A concerns that may arise due to reactions between ROSs and nuclear material. ROSs may be introduced through a number of pathways, including atmospheric ingressions, selective depassivation of structural alloys, and inadequate salt purification.⁹ Previously reported efforts towards the characterization of ROSs largely yielded imprecise physicochemical properties that ultimately complicate quantitative analysis of corrosion rates and material tracking. Using a model system, fundamental studies of oxide-containing molten salts were conducted. These studies were coupled with numerical simulations to provide accurate and precise measurements of dissolved oxides in molten salts.

2. Survey of Historical and Contemporary Molten Salt Loops and Flow Systems

In this section, a survey of historical and contemporary molten salt loops and flow systems is provided to contextualize Argonne's pumped actinide salt loop. Henceforth, discussions pertaining to "loops" refers to a closed convection system wherein molten salt can flow circuitously. In contrast, "flow systems" refers to convective configurations wherein molten salt is transported from one holding tank to another. It is important to emphasize that the discussion presented herein only serves as an overview of some salt loops and flow systems, and is not meant to provide an exhaustive summary of all existing technologies. A table summarizing the content provided in this section is given in Appendix I.

2.1. Historical Overview and Modern Needs

Molten salt flow systems relevant to nuclear applications date back to the 1950s when a series of thermal¹⁰ and forced^{11–13} convection test loops were constructed at Oak Ridge National Laboratory (ORNL) to quantify corrosion rates of metallic alloys in actinide-bearing Be-based molten salts. Typical photos of loops constructed during this era are shown in Figs. 1 and 2. The results from these molten salt systems culminated in the operation of the Aircraft Reactor Experiment (ARE)^{14,15} and the Molten Salt Reactor Experiment (MSRE),¹³ a circulating molten LiF-BeF₂ (FLiBe) loop that contained ZrF₄ and fueled with UF₄ or ThF₄.¹³ Studies conducted during this time were aimed at characterizing the effects of process parameters on alloy corrosion rates and to characterize the efficacy of practical MSRs. Operating conditions such as salt flow rate, process temperatures, and redox control systems were of particular interest. Technological advancements, such as high temperature pumps, seals and sampling capabilities, were developed as a result of the work conducted during this time.^{15,16}

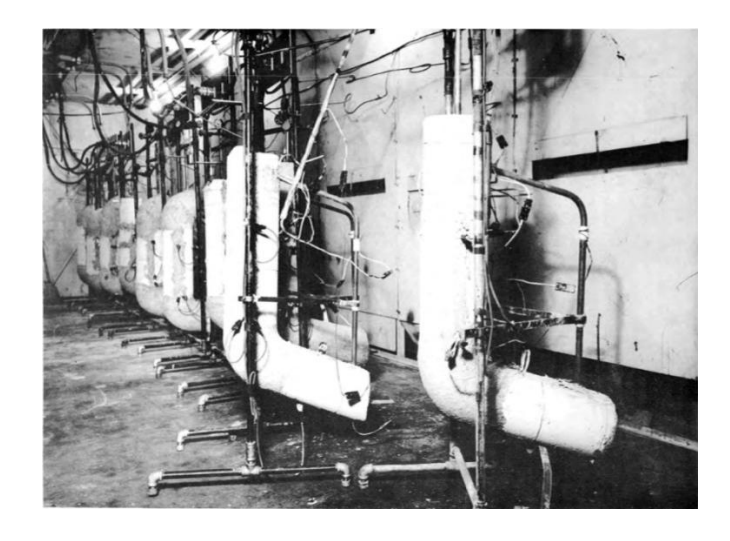


Figure 1. Thermal convection loops operating as part of the Aircraft Reactor Experiment¹⁴

Figure 2. Pumped loops operating as part of the Aircraft Reactor Experiment¹⁵

The large number of loops and flow systems constructed during the 1950s and 1960s enabled immense increases in the knowledge of molten salt chemistry, corrosion, operations, and maintenance protocols. While a wealth of knowledge was gained during these extended at-temperature testing campaigns, modern occupational health and safety regulations restrict capabilities for fabricating and testing large numbers of open floor experiments using hazardous salts relevant to MSRs; as such, the production and operation of a large number of loops containing radiological and Be-bearing salts in a manner akin to the photos above is impracticable.

Nonetheless, the advent of modern technologies, coupled with the wide range of potential MSR taxonomies, underscores the need for inexpensive, modular, and nimble testing capabilities. The proceeding subsections therefore highlight the engineering- and pilot-scale efforts aimed at reestablishing the previously-achieved scale and ubiquity of MSR testing platforms in the U.S. Subsequent sections will present Argonne's work in FY25 to develop forced convection actinide-bearing molten salt loops that enable modular testing of MSR-relevant technologies.

2.2. Contemporary Molten Salt Flow Loops

Contemporary efforts to produce molten salt testing platforms have been pursued at a variety of institutions. At ORNL, two non-radiological forced convection molten salt loops have been constructed and intermittently operated, namely the Liquid Salt Test Loop (LSTL) and the Facility to Alleviate Salt Technology Risks (FASTR). Each of these loops were designed to simulate industrial MSR conditions in the absence of radiological material. As such, they are equipped with various heat exchangers, purification vessels, and instrumentation ports. The LSTL was first operated in 2016 and was constructed to support testing campaigns using molten LiF-NaF-KF (FLiNaK). During FY23 operations, a variety of activities were conducted on the LSTL including those involving Argonne's electrochemical sensors. ¹⁷ Operations were paused in FY23 to allow for maintenance activities aimed at addressing a suspected gas space leak, and the loop has been out of service ever since. As with Argonne's pumped actinide salt loop, FASTR utilizes a centrifugal pump to transport molten chloride (NaCl-KCl-MgCl₂) salt. The system is capable of housing 250 kg of salt and operating at temperatures up to 725°C. To mitigate the potential for structural material corrosion induced by atmospheric ingressions, FASTR was primarily constructed from Hastellov® C-276.18 In FY24, sensor testing studies were conducted using technologies developed by Argonne and Pacific Northwest National Laboratories. Additional collaborative testing campaigns are ongoing in FY25. ORNL has also operated a variety of thermal convection loops over the past decade; ^{19,20} some of these tests included inline salt chemistry monitoring provided, for example, by Argonne's electrochemical sensors.

In addition to the in-glovebox molten salt flow loop discussed in this report, Argonne is in the beginning stages of operating its Separate Effects Loop (SEL), an engineering-scale molten chloride flow loop. This loop is designed for thermal hydraulic and molten salt technology studies and is capable of operating at temperatures up to 725°C. The SEL is equipped with an in-house salt purifier and scrubber, salt-to-air heat exchangers, and corrosion control capabilities. Moreover, the facility includes a number of process monitoring and automation technologies such as Argonne's electrochemical sensors and ILEX© software. Purification of the salt is underway, and test matrices have been established as the SEL nears its final operational state.

In FY25, Idaho National Laboratory (INL) announced the initiation of a thermal convection loop to study molten chloride salts. This loop houses a triple bubbler and electrochemical sensor to support process monitoring of a non-radiological salt. In contrast, the Molten Salt Tritium Transport Experiment (MSTTE, currently under development at INL) is a forced convection molten salt loop intended to study the transport of hydrogen isotopes in molten fluoride salts. Convection capabilities are maintained through external connection of the MSTTE to a salt tank and pump assembly constructed by Copenhagen Atomics. ^{22,23} Future experimental efforts will primarily focus on using molten FLiNaK and deuterium as surrogates for FLiBe and tritium, respectively. ²² Construction of the MSTTE loop is ongoing in FY25.

The Molten Salt Test Loop (MSTL) facility is an industrial-scale nitrate salt test loop constructed at Sandia National Laboratory for concentrating solar power.²⁴ This facility is capable of flowing up to 400 gallons per minute (gpm) and operating at temperatures up to 600°C. Efforts to restart the facility from frozen medium-term storage have been initiated in FY25 and are expected to be complete by 2026.

Molten salt loops have also been developed at a variety of universities. For example, a natural convection loop at the University of Wisconsin was previously constructed to study the flow of molten FLiBe. ²⁵ This loop can operate at temperatures up to 800°C and under non-isothermal conditions, albeit with low flow rates due to natural convection-driven processes (~ 0.25 gpm). Collaborations with TerraPower in

investigating corrosion of alloys in small-scale molten chloride flow loops are ongoing. Many other molten salt flow systems have also been operated at the university.²⁶

A pumped salt loop was constructed at Virginia Polytechnic Institute and State University to enable corrosion studies in a molten chloride salt (NaCl-KCl-MgCl₂).²⁷ The loop was capable of operating at 650°C and at a flow rate of 0.7 gpm. Persistent salt and gas leakage from this loop was noted, and operations were paused due to ongoing safety concerns. The current operational status of this loop is presently unknown.

Massachusetts Institute of Technology (MIT) is collaborating with other universities and ORNL to construct a pumped salt loop for the MIT reactor.²⁸ The project was initiated in 2020. It presently includes contributions from the University of California, Berkeley to develop electrochemical probes to support redox monitoring and control of the salt, and from North Carolina State University to monitor off-gas composition. ORNL will also support the loop development. Presently, non-radioactive loop operation using molten FLiNaK was planned for 2025 to inform the eventual loop installed on the MIT reactor.²⁹

In September 2024, the U.S. Nuclear Regulatory Commission (NRC) issued a permit allowing for Abilene Christian University (ACU), in collaboration with Natura Resources, to begin construction on the Molten Salt Research Reactor (MSRR).³⁰ The MSRR is intended to support academic research efforts through the construction of a 1 MW_{th} molten FLiBe loop containing dissolved High Assay Low Enriched Uranium fuel. Industrial partnership with Copenhagen Atomics included the purification and transfer of 250 kg of molten fluoride salts to ACU. Rapid and modular testing of MSR technologies and operating conditions will be challenging on account of the potential exposure risks associated with Be-based salts. A variety of test loops are planned or already in operation to support the development of the MSRR.³¹

Commercial MSR vendors have also constructed and operated molten salt flow loops. In January 2024, Kairos Power announced the thousand-hour long operation of a FLiBe molten salt loop that was capable of flowing 3,000 gpm of salt.³² A follow-up ETU is also planned for construction. Construction of the fluoride salt-cooled Hermes Low-Power Demonstration Reactor (35 MW_{th}) is currently underway and will ultimately serve to complement the eventual Hermes 2 reactor (20 MW_e followed by 140 MW_e). Engineering-scale salt test loops (STLs) have been constructed using molten FLiBe as the flowing medium. Among the technologies tested in these loops were Argonne's flow-enhanced electrochemical sensors³³ and corrosion control mechanisms.

TerraPower and Southern Company have previously announced the completion of the Integrated Effects Test molten salt loop. This loop is an externally heated, non-radiological forced convection loop intended on informing the development of TerraPower's Molten Chloride Fast Reactor.³⁴ TerraPower has also operated a wide range of micro-loops to study material performance and other aspects of molten salt operations.³⁵

Copenhagen Atomics has constructed and delivered portable molten salt forced convection loops to numerous institutions, including universities and national laboratories.³⁶ Their loops are constructed from stainless steel and are equipped with highly purified fluoride salts. The construction of these loops, combined with data provided by pump customers, are intended to inform the eventual construction of their fission and breeder reactors. Construction of a prototype non-fission MSR is expected to be completed in 2025, commercial reactors by 2028, and ultimately a breeder reactor by 2034.

Other international efforts aimed at the development of molten salt loops should also be noted, although a detailed survey of these efforts is beyond the scope of this work. Several natural and forced convection loops have been constructed and operated at the Shanghai Institute of Applied Physics, Xi'an Jiaotong University, and others.³⁷ The operational time of these loops has been reported to be in excess of 10,000 hours. The loops utilized molten nitrates and fluorides to study heat transfer and corrosion phenomena. The Shanghai Institute of Applied Physics has also operated a thorium-based MSR for extended periods that was refueled without the need for a reactor shutdown.³⁸ Studies are ongoing to develop molten salt technologies, evaluate corrosion-resistant materials and tests of online salt monitoring capabilities in flowing salt systems.

2.3. Contemporary Molten Salt Flow Systems

Argonne has constructed and operated a number of molten salt flow systems, including the Modular Flow Instrumentation Testbed (MFIT) which has enabled sensor and technology testing for the past four years.^{39–41} Iterations of this system have been designed and built to accommodate a range of molten salt chemistries and technologies. For example, the MFIT is capable of flowing up to 15 L of actinide-bearing salt through pressure-driven forced convection.⁴⁰ A scaled-down iteration of the MFIT was constructed to provide operational feedback for advanced electrochemical sensors and instrumentation to be used in the MFIT.³⁹ In FY24, electroanalytical sensing techniques, coupled with numerical simulations, were used for the first-known precise measurement of high concentrations (72 wt% U) of actinides in fuel salts.⁴⁰ These technological developments further supported ongoing activities in FY25 towards developing sensors capable of monitoring complex flowing salt compositions. Several miniature MFITs have also been operated at Argonne over the past five years with a variety of salts.⁴¹

Other tank-to-tank flow systems similar to Argonne's MFIT have been operated in industry and national laboratories. In 2017, ORNL reported on the construction of a tank-to-tank molten salt flow system⁴² that intended to use dynamic weighing to track fluid flow through the transfer line. As of this writing, the operational status and data output from this system is unclear.

Kairos previously constructed the Instrumentation Test Unit (ITU) to further develop and study the performance of technologies intended for deployment in their large-scale flow loops. ⁴³ The ITU consisted of tank-to-tank molten FLiNaK salt flow through a transfer line equipped with several process monitoring technologies. Since the construction of the ITU, Kairos has transitioned into the large-scale molten salt flow loops as described in Section 2.2.

Alongside sensor testbeds, Argonne also operated a multiphase flow system for testing of cyclonic separations and filtering technologies.⁴⁴ This work was aimed at separation of solid-phase particles that are known to accumulate in MSRs. Other such multiphase systems have been operated at various institutions. For example, ORNL has previously injected Kr and Ar gas to study bubble formation in bench-top experiments and forced convection loops.⁴⁵ In another study, Texas A&M University studied bubble recirculation in a natural convection molten salt loop through Ar gas injections.⁴⁶

The Shaft Seal Test Facility (SSTF) at the University of Michigan serves to evaluate both the performance of high temperature seals and inert gas consumption rate of molten salt systems.⁴⁷ The SSTF operates by pumping 32 kg of molten FLiNaK salt from a primary holding cell and into a secondary vessel through salt transfer lines. It has been reported that, as of July 2025, the SSTF has operated for 2,300 hours.

2.4. Assessment of Existing Flow Loops and Flow Systems

The range of existing loops and flow systems were assessed based on metrics established for deployment of practical MSRs. The metrics included valuations of methods to induce flow (thermal vs. forced convection), modularity, salt chemistry (*i.e.*, radiological vs. non-radiological), system size, flow conditions, scalability, and operational status. An ideal testbed for molten salt technology is a modular, forced convection flow loop that integrates radiological molten salts under realistic flow conditions. Furthermore, to accelerate the deployment of advanced nuclear reactors, forced convection loops that have demonstrated near-term operational readiness are of particular importance. Results from the detailed assessment of the existing systems discussed in Sections 2.2 and 2.3 are outlined in Appendix I. Argonne's pumped actinide molten salt loops, which have been designed to satisfy key performance metrics for an ideal MSR testbed, will be discussed in more detail in proceeding sections of this report. As shown in Appendix I, other systems operated in industry and elsewhere have also able to meet many of these metrics.

3. Glovebox Infrastructure

Argonne's actinide flow loops are designed to be installed into the Molten Salt Flow Systems glovebox located in the Molten Salt Technology Development Laboratory. A photo of this glovebox is shown in Fig. 3. A rendering of the glovebox and installation location for the loops is shown in Fig. 4. This glovebox had been used previously to house a variety of other experimental apparatuses including a modular test bed for molten salt sensors, ^{39–41} a pyrocontactor system that centrifugally mixed streams of liquid metals and molten salts in order to effect separations, and a test apparatus used to study oxygen and moisture ingressions into salts. ⁴⁸

Integration of molten salt flow loops into gloveboxes is advantageous from a material handling standpoint but presents several challenges with respect to thermal management, pressure safety, gas purification, and electrical power. In FY25, the glovebox received a variety of upgrades to manage these issues. Additional modifications are planned for FY26 prior to operations of the loop. The section below describes some of the existing and upgraded infrastructure that was implemented to accommodate the loop.



Figure 3. Photograph of the Molten Salt Flow Systems Glovebox

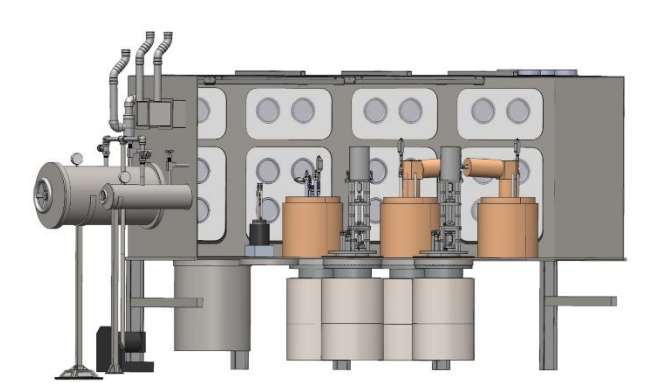


Figure 4. Rendering of the Molten Salt Flow Systems Glovebox showing location of loops and other flow apparatus

3.1. Pressure Control and Pressure Safety

In order to permit handling of large quantities of radiological materials, the glovebox is maintained at negative pressure. Fig. 5 shows the permissible range of pressures that has been adopted for the box based on historical practices and guidelines from the American Glovebox Society. Flow systems installed within the glovebox complicate maintenance of this pressure range as stored energy could lead to excursions outside of the permitted range. While low- and high-pressure oil bubblers are present as a backup to accommodate unintended excursions, the flow systems and other components were designed such that the glovebox pressure would be maintained in the proper range regardless of any instantaneous pressure releases from the equipment.

Safety calculations for the loops were conducted to confirm the adequacy of the design with respect to pressure release scenarios including (1) broken piping with instantaneous gas release, (2) pressure excursions caused by the flow of gas into the box from pressurized gas supplies, and (3) pressure excursions caused by the use of vacuum pumps located outside of the box. These

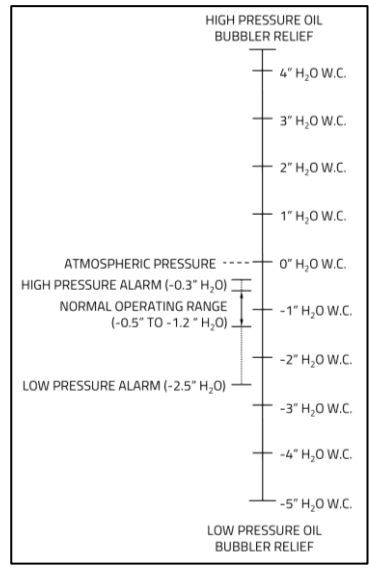


Figure 5. Pressure range for the negative pressure glovebox

calculations were simplified by the fact that the in-glovebox loop designs do not contain pressure vessels (as the molten salt crucible is open to atmosphere) and instead only includes piping that is at pressure. The total stored energy is therefore low. All the calculations showed that the systems that are being prepared for installation satisfied pressure safety requirements.

3.2. Gas Purification

Adequate gas purification is important for the in-glovebox flow loop as the vessels are open to the glovebox's argon atmosphere. Oxygen and moisture purifiers were therefore included to maintain the glovebox at less than 10 ppm O₂ and 10 ppm H₂O. The existing glovebox purifier consisted of an MO-120 Dri-Train manufactured by the Vacuum Atmospheres Company.⁴⁹ This purifier is capable of operations at 120 cfm and was installed in approximately 1990. The system had proven capable of maintaining the glovebox atmosphere at suitable levels over three decades of operations, but the increased maintenance requirements of the old purifier along with a need for improved control of the atmosphere necessitated the installation of a new purification system. Two new Vacuum Atmospheres Nexus modular purification units were therefore procured to support the MSR Campaign activities and other programmatic activities in the glovebox.^{40,50} These purification units, in parallel, can purify up to 400 cfm of the atmosphere, enabling turnover of the entire glovebox atmosphere in under 30 seconds. All ancillary items for the updated purification system have been procured, and the new units are being prepared for installation in early FY26. Loop operations can still occur using the existing purifier, but higher temperatures and longer-term operations will be permitted once the new system is installed.

3.3. Thermal Management

The glovebox's existing thermal management system consisted of multiple subsystems including jacketed chilling of the discharge and return piping, an internal heat exchanger within the MO-120 purifier, and cooler coils on the glovebox flanges. Photos of these individual systems are included in Fig. 6. The heat rejection capacity for these systems was provided by the lab's recirculating cold-water supply or by a separate refrigerated loop for the jacketed chillers. The combined systems were designed to maintain the

glovebox atmosphere at less than 50°C to ensure safe operations. Also, seals including O-rings at various locations within the glovebox have established temperature limits to ensure the achievement of suitable leak rates.

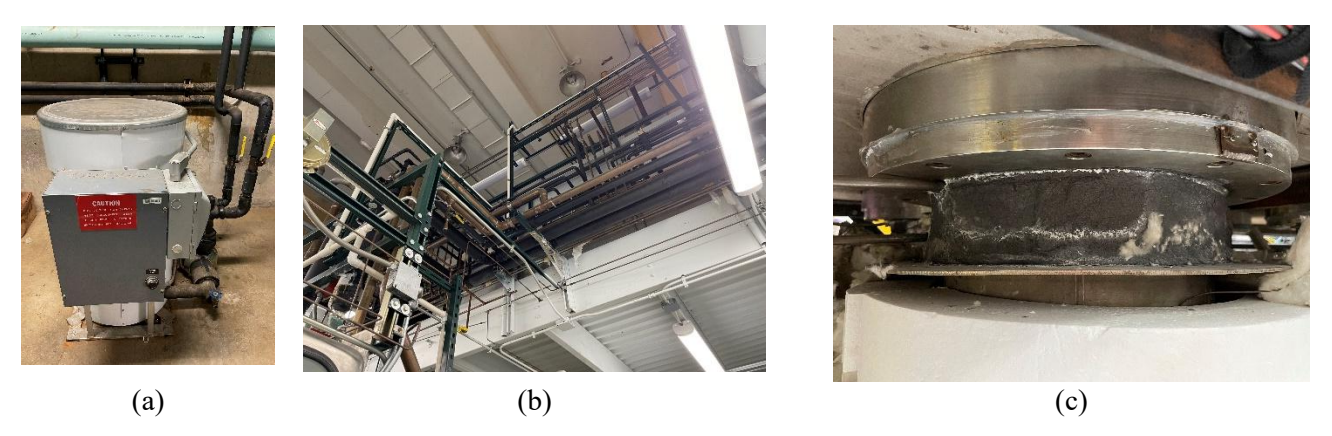


Figure 6. Existing glovebox cooling subsystems including (a) chiller located on service floor, (b) mezzanine level cooling jackets for the return and discharge, and (c) flange cooling coils embedded in heat transfer media

Updates to this existing thermal management system were necessitated by the increased thermal load of the flow loop. The largest planned upgrade is the procurement of a Vacuum Atmospheres DK-10E inline glovebox cooler. This system is capable of removing up to 1.5 kW of heat from the inert argon environment. An additional chiller has also been procured to augment the recirculating lab cold water that is currently used to cool the glovebox flange, although preliminary calculations indicate the existing coolant will be sufficient to maintain proper flange temperatures (see Section 4.2). Options for switching the glovebox to an inert helium atmosphere are also being explored due to the poor heat transfer performance of argon; the cost of helium, however, may be prohibitive.

3.4. Salt Purification

Engineering-scale salt synthesis and purification capabilities were also established within the glovebox in FY25 to enable production of sufficient salt to support loop operations. Co-location of the salt purification system with the loop eliminates the need for material transfers and ensures maintenance of the targeted salt purity level. The salt purification system and procedures were developed under the Advanced Reactor Safeguards and Security program, but the system will be used to support salt production for several projects.

The purification system, shown in Fig. 7, makes use of uranium metal feedstock. ZnCl₂ is then used as a chlorinating agent to generate UCl₃ within the solvent salt. Reduced zinc metal is distilled from the system and captured in scrubber media. The overall approach has been used to generate several kilograms of salt thus far; in FY26, serialized production of batches at a scale of approximately 3 L/batch will be performed to generate the salt needed for the loop.



Figure 7. Photo of salt purification system using uranium metal feedstock. Fabrication of the salt purification system was funded by DOE NE-5's Advanced Reactor Safeguards and Security program

4. Design and Construction of Pumped Loop Assemblies

In this section, we outline the design, testing, and construction of the molten salt pumps, loops, and supporting equipment completed in FY25. A brief discussion regarding the preparation of additional process monitoring technologies for in-glovebox operation planned for FY26 is also provided.

4.1. Pump Design

Together with feedback from Argonne, High Temperature Systems Design, LLC designed a molten salt pump for in-glovebox operation. It was designed such that insertion into the radiological glovebox outlined in Section 3 could progress through the antechamber with minimal detriment to the inert atmosphere. Fig. 8 shows renderings and photographs of the pump's three segments along with their approximate dimensions. The motor (Segment 3, 1 HP, Weg Electric Corp., model no.: 00118ET3ER143TC-W22) was procured through readily available commercial resources. Segment 2 served as the coupler between the motor and the remainder of the pump. Segment 1 contained the discharge and return tubes. These tubes connect to the molten salt loop through liquid-tight Swagelok® fittings. This section also contained the heat shield pack, pump impeller and instrumentation ports for modular insertion of process monitoring and control technologies. It should be noted that all salt-wetted contact points were constructed using 316 stainless steel (316 SS). Moreover, because the pumped actinide salt loops operate at ambient pressures, the application of American Society of Mechanical Engineers standards for material compatibility, construction (e.g. welding), and non-destructive examination of pressure vessels is not necessary.

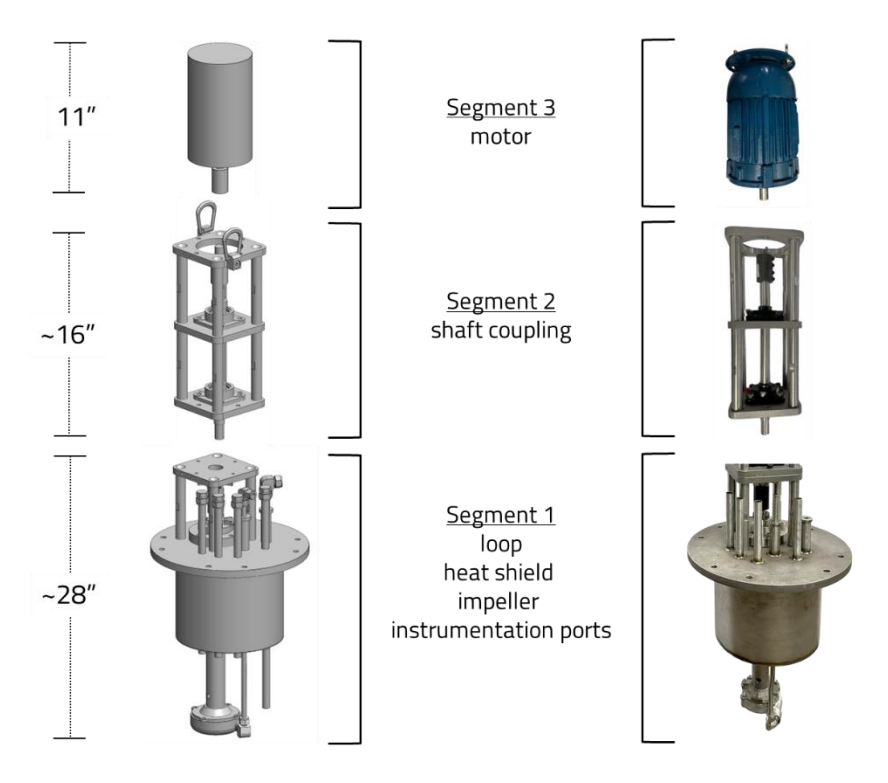


Figure 8. (left) Rendering and (right) images of the partitioned molten salt pump

Fig. 9 shows a rendering of the pumped actinide loop assembly's cross-section in the well alongside a photo of the pump installed in the radiological glovebox. Here, we limit the discussion to the pump as details regarding the ancillary equipment labeled on the rendering are provided in subsequent sections. The pump's mounting plate in Segment 1 is equipped with eight through-holes that were designed to affix the pump onto a secure platform. As such, a stand composed of low profile 316 SS Unistrut paired with vibration dampeners was secured to channels welded onto the glovebox floor. Moreover, the ports on the pumps were designed in order to maintain operating temperatures and process monitoring capabilities.

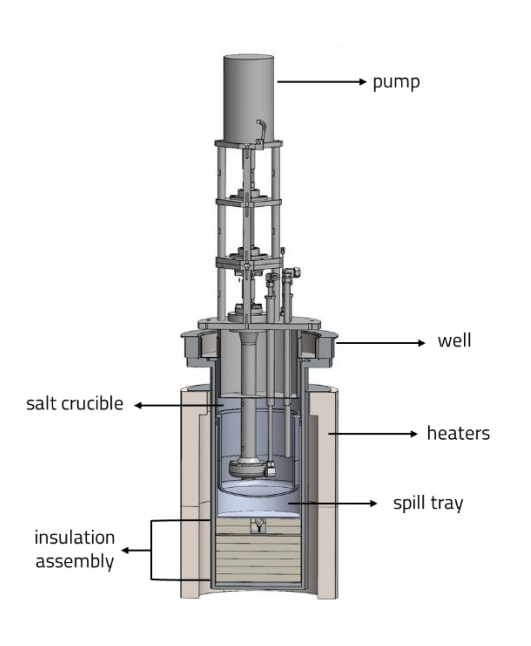




Figure 9. Cross section rendering and photograph of pumped actinide molten salt loop seated in a radiological glovebox well

Two pairs of Watlow clamshell heaters (VS416A12S and VS316A12S) were procured to provide external heating to the well as shown in Fig. 9. It should be noted the lower clamshell pair (VS316A12S) was equipped with heating elements that may be utilized as future heating needs evolve; however, preliminary operational plans involve its use as support for exterior-to-glovebox insulation. The installation of thermocouples and insulation jacketing will be necessary to enable safe operation of the pump in FY26.

4.2. Supporting Pump Equipment

A number of ancillary equipment needed to support loop operations were designed and constructed in FY25. Renderings of these equipment are shown in Fig. 10 and were intended to improve the safety and reliability of the loop during at-temperature operation.

The actinide-bearing molten salt will be loaded into custom-designed salt crucibles constructed from 316 SS. As seen in Fig. 9, the crucible was designed for seating on the glovebox well flange. Holes tapped at 45° intervals along the lip of the crucibles allow for adaptable and centered lifting capabilities using the glovebox's overhead chainhoist used during crucible installation or removal. The upper body of the crucible was sized to fit within the well and around the heat shield portion of the pump. Maintaining radial distances in excess of 0.1" mitigated the potential of unintended detrimental physical contact as a result of thermal expansion. The upper and lower portions of the salt crucibles were connected through full penetration butt welds and a 3/8" thick 316 SS metal plate. At-temperature molten salt will be housed in the lower portion of the crucible wherein a Schedule 40 pipe and pipe cap were used. Wall thicknesses and weld types were chosen to minimize the potential for salt egression from the crucibles and into the wells. Note, from Fig. 10, each crucible can maintain approximately 15 L (i.e., 25 – 30 kg) of molten salt while still operating at-temperature in the glovebox. Larger-scale versions of these loops are also possible using the larger furnace wells present in neighboring gloveboxes.

The insulation annulus was designed to provide added insulation to the glovebox flange. It was constructed using 316 SS, and the gap was packed with alkaline earth silicate ceramic fiber pipe insulation (8 lbs/ft³, 0.73 BTU at 800°F). Wall thicknesses (0.06") were chosen to minimize conductive heat transfer while maintaining the component's structural integrity during welding and construction.

The inherent containment capabilities afforded by in-glovebox operation mitigate the risks and consequences arising from off-normal scenarios wherein salt extrusion from the intended flow path may occur. Nonetheless, we designed a salt spill catch tray to eliminate the potential of infrastracture damage that may ultimately lead to operational pauses. A schematic representation of the catch tray is shown in Fig. 10. The tray was constructed using 316 SS and designed to rest on the upper portion of the insulation assembly. A handle was welded onto the inner floor of the catch trays to facilitate installation and removal as necessary.

Note in Fig. 9, the insulation assembly pack was installed at the base of the glovebox well to maximize heating efficiency and ensure wall temperatures are maintained within their intended design constraints. The insulation assemblies were custom-machined using rigid 1" thick calcium silicate insulation (40 lbs/ft³, 0.8 BTU at 800°F) and secured with 0.25" thick 304 SS plates. An eyebolt was included in the assembly to enable maneuvrability using the glovebox's overhead chainhoist.

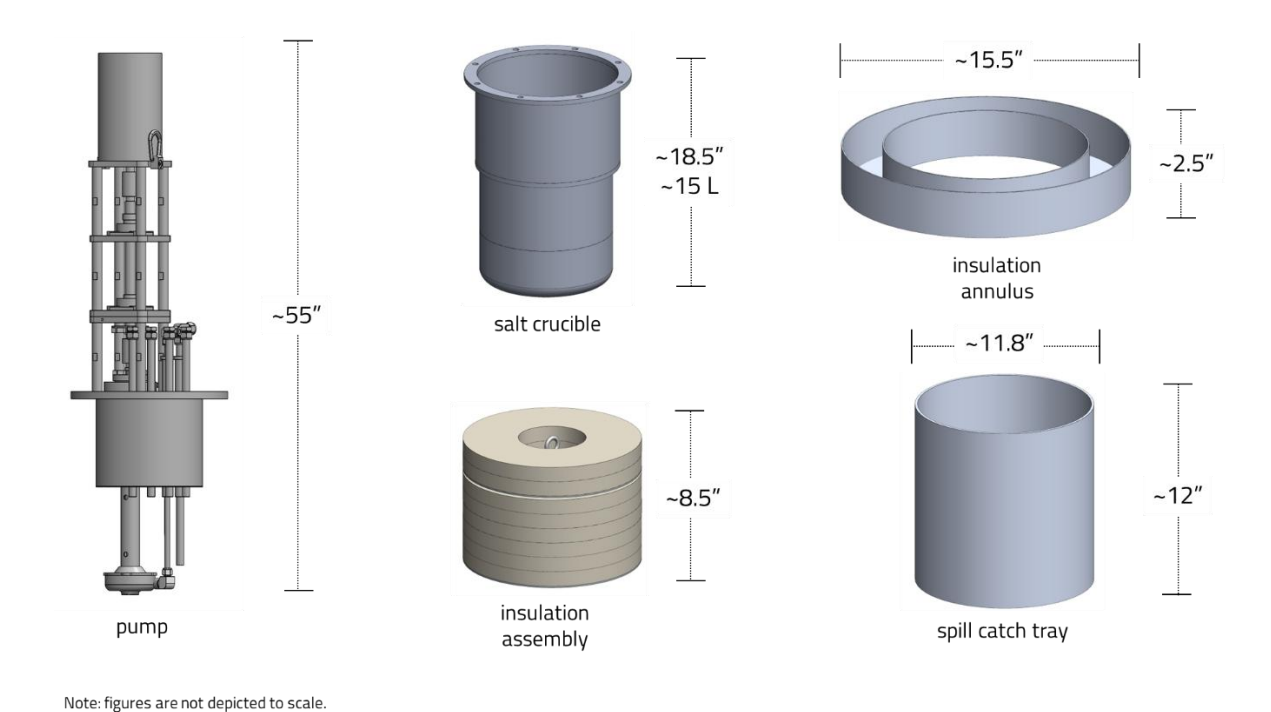


Figure 10. Renderings of the assembled pump along with ancillary equipment such as the salt crucible, insulation assembly, annulus, and the spill catch tray. Dimensions listed are approximate and renderings are not shown to scale

Provisional simulations were conducted of the system to ensure the salt remains at the target operating temperature while maintaining (1) sufficient cooling to the glovebox infrastracture and (2) operator safety. Fig. 11 shows the thermal profile of the system assuming stagnant flow conditions and salt temperatures in the 550-750°C range. It is expected that the salt temperature will homogenize under convective

conditions. It should be noted that we also assumed the cooling coils located on the exterior of the well are providing adequate cooling capabilities such that the glovebox floor and flange remain at 80°C. In practice, thermal management capabilities of the bulk glovebox atmosphere, coupled with added insulation will help to maintain all glovebox infrastructure within their intended operating temperatures. Additional simulations will be conducted in FY26 to capture transient and convective heat transfer conditions.

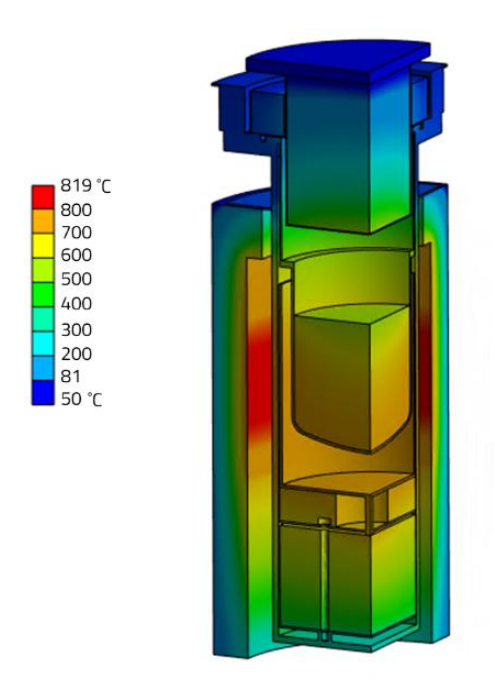


Figure 11. Steady-state temperature contours for the furnace well with molten salts, pump and supporting equipment assemblies

4.3. Initial Pump Performance Testing with Water

It was critical to collect performance data of the pumps using a water test loop prior to installation and operation of the pump in the radiological glovebox. This activity informed operational modes and details that would otherwise remain unknown during molten salt pump operation, particularly as they relate to cavitation performance⁵¹ of a molten salt pump. A piping and instrumentation diagram (P&ID) of the water test loop is shown in Fig. 12 along with a photo of the physical setup used to produce pump performance curves.

The stand on which the pumps and loops were seated was constructed from T-slotted framing equipped with vibration dampening feet and pads. To prepare for testing, the pump's discharge and return lines were fully submerged in the basin containing deionized water. A variable frequency drive (VFD, Schneider Electric, model no.: ATV12H075F1) was used to control the motor and shaft speeds. Inline pressure gauges were placed on the discharge and return lines of the loop to determine pressure differentials needed to construct performance curves. A metering valve was also installed inline to modulate flow at a specific VFD frequency. The flow rate was recorded using a magnetic-inductive flowmeter (ifm electronic, model no.: SM6604). A vibration monitor (ifm electronic, model no.: VNB001) was also installed on the pump to characterize the pumps' vibration levels prior to installation and operation with molten salts.

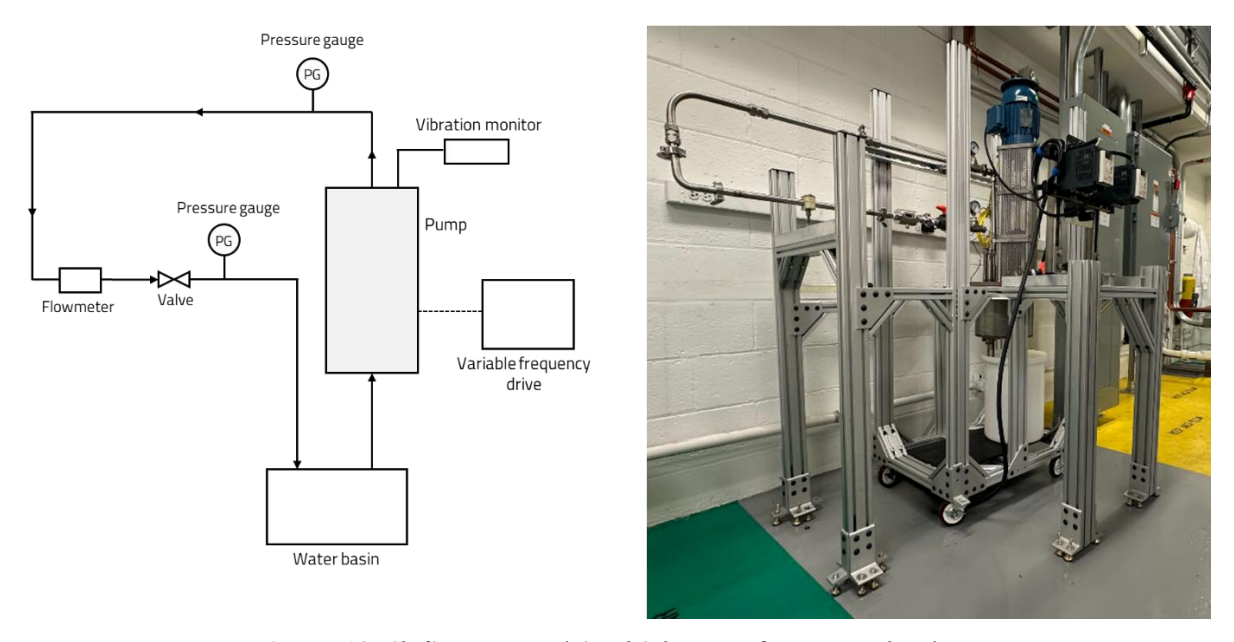


Figure 12. (left) P&ID and (right) image of water testing loop

A photo depicting the VFDs used for water testing is shown in Fig. 13. Note, the mounting distance between the two VFDs was maintained at 6", *i.e.* well beyond the vendor's recommendation for Type A mounting (2" distance) in ambient conditions, owing to the eventual installation in an argon atmosphere. A combination of strut channels and vibration dampeners were used to minimize the potential for vibrational stresses disaffecting the lifetime or reliability of the VFDs. During operation, care was taken such that all NRTL electrical safety codes (e.g. finger-safe configurations) were maintained.



Figure 13. Variable frequency drives used for pump operation

It was of particular importance during this testing campaign to relate VFD settings to rotation speeds of the pumps' shafts. As such, a tachometer (Extech Instruments, model no.: 461920) was used to measure RPM as a function of the user-input VFD frequency. The results of this activity are shown in Fig. 14a. As expected, the relationship between the rotation speed and VFD frequency were linear and crossed through the origin. Care was taken such that the vendor's specification of the maximum motor rotation speed (1760 RPM) was not exceeded. Vibration levels at each of these frequencies were also recorded and representative data sets are shown in Fig. 14b. The dotted lines on Fig. 14b correspond to vibration zones set by ISO 20816 for Class I motors. Zone A and Zone B are classified as newly commissioned and unrestricted operation, respectively. For additional reference, Zone C corresponded to restricted operation and finally, Zone D outlines vibration levels where damage is expected. Note, the vibration velocity of the motor remained well within unrestricted operational zones.

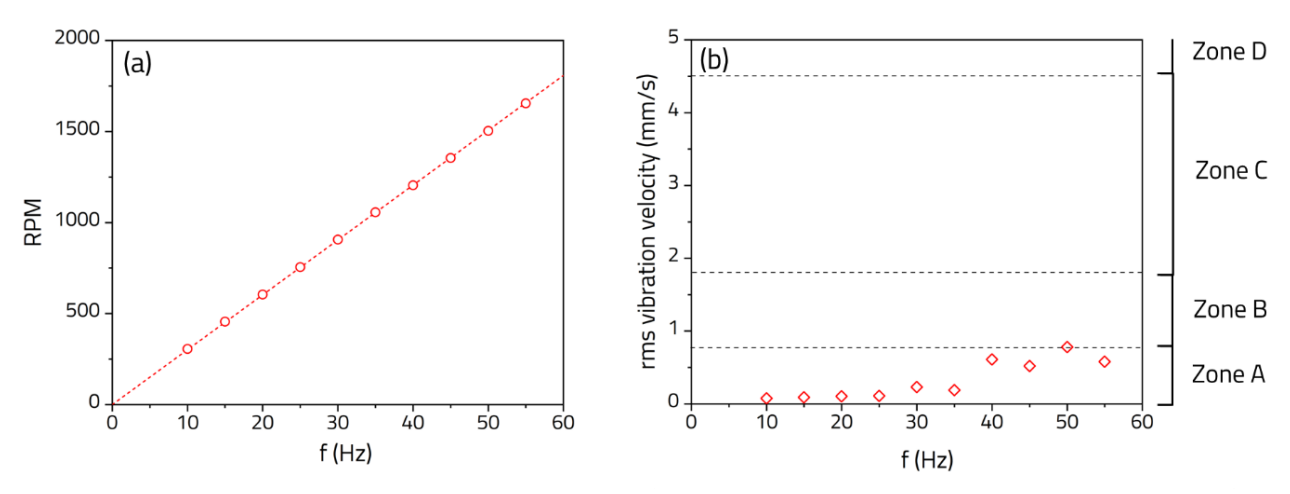


Figure 14. (a) Measured RPM and (b) rms vibration velocity as functions of VFD frequency. In panel (b), vibration zones are labeled per ISO 20816 for Class I machines

Using the water testing loop shown in Fig. 13, we evaluated the performance of the pumps at various operating conditions. The results can be seen in Fig. 15. Note, the flow rate was modulated using both the metering valve and by varying the VFD's frequency. The precise determination of ideal operational modes for flowing molten salts is difficult to assess solely from water testing. Nonetheless, in accounting for head pressure and vibrational changes associated with molten salts relative to water, ideal operating frequencies and flow rates are expected to lie within 40 - 50 Hz and 1 - 2 gpm, respectively. The modularity offered by the in-glovebox flow loops allows for localized variance of Reynolds numbers to simulate variable fluid flow conditions as needed.

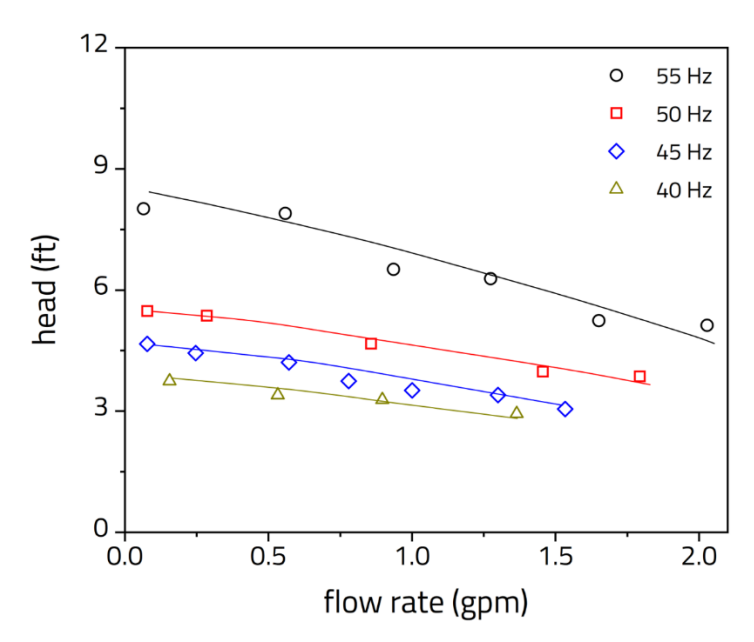


Figure 15. Pump head pressure as a function of VFD frequency and flow rate

Efforts and activities are ongoing to prepare the loop with sufficient safety features and process monitoring equipment to enable operation in FY26. One such feature entails the integration of a seal guard around the shaft to protect operators from unintended contact with the rotating shaft. Furthermore, because the well heaters will be operating at temperatures in excess of 600°C, sufficiently thick insulation will need to be jacketed around the heaters to ensure operator safety. The ubiquitous use of thermocouples throughout the pump assembly will support efforts to maintain controlled operations. Additional safety measures such as the integration of overtemperature controllers, interlocks, and splash guards will also be included prior to operation.

5. Characterization of Reactive Oxide Species

To further support the planned loop operations, Argonne has continued to develop electrochemical sensors to enable proper monitoring and control of the molten salt equipment. To ensure successful long-term performance, it is of particular importance to sufficiently identify chemical speciation of ROSs in molten salts such that effective and targeted corrosion control mechanisms may be deployed. Towards that end, electrochemical measurements were taken in salts containing known amounts of ROSs. In practical systems, ROSs propagate due to a number of factors including atmospheric ingressions and residual bulk impurities.^{5,9} The results presented in this section summarize the simulation-informed experimental efforts conducted in FY25 aimed at characterizing these species in a model fluoride-based molten salt. Additional detail and content pertaining to this work may be found in the publication by Shaheen and Hoyt.⁹

Experiments were collected using square wave voltammetry (SWV) to deconvolute overlapping electrochemical signals. Theory governing this technique dictates that the following relationship between the peak difference current (ΔI_D) and measurement frequency (f) is:⁵²

$$\Delta I_{\rm p} = \frac{nF\sqrt{2fD}AC_{\rm b}}{\sqrt{\pi}}\psi$$
 [1]

where n is the number of electrons, F is Faraday's constant, D is the diffusion coefficient, A is the electrode's area, C_b is the bulk concentration, and ψ is the dimensionless peak current. Uncompensated Ohmic resistance effects (IR $_{\Omega}$) are known to attenuate voltammograms such that a non-linear relationship between the peak difference current and the square root of frequency is observed. Therefore, to characterize reaction mechanisms, SWVs were conducted using positive-feedback IR $_{\Omega}$ compensation. It should be noted that, while effective for academic purposes, positive-feedback IR $_{\Omega}$ compensation is not feasible in industrial applications. As such, we used the post-experimental correction factors 7,9,54 derived from numerical simulations conducted in FY245 to calculate physicochemical properties associated with the following peroxide-mediated reaction:

$$20^{2-} \to 0_2^{2-} + 2e \tag{2}$$

5.1. Experimental Methods and Simulation Setup

All experiments and salt preparation were conducted in a boron nitride crucible located in an inert atmosphere glovebox. Lithium fluoride (LiF, ≥99%, Sigma-Aldrich), potassium fluoride (KF, 99%, Sigma-Aldrich), sodium fluoride (NaF, ≥99%, Sigma-Aldrich) and lithium oxide (Li₂O, 97%, Sigma-Aldrich) were all individually baked at 450°C for 6-8 hours to remove residual moisture. The base fluoride eutectic was synthesized by mixing the appropriate amounts of LiF, KF, and NaF to maintain a 46.5–42–11.5 molar ratio. The salt was then heated at a ramp rate equal to 4°/min to experimentally relevant temperatures (550, 600, 650, 700°C).

Electrochemical data reported herein were collected using a standard three-electrode configuration. The working, reference, and counter electrodes were 1 mm wires composed of either silver (99.9%, Sigma-Aldrich) or tungsten (99.95%, ThermoShield). The immersion depth of the working electrode was controlled using a vertical translator. Square wave voltammograms were collected using a Gamry Interface 5000E potentiostat and a Gamry Reference 3000 potentiostat for positive-feedback IR $_{\Omega}$ compensation. The pulse and step potentials in SWVs were 12.5 mV and 2 mV, respectively. Impedance measurements were collected using the potentiostatic electrochemical impedance spectroscopy (PEIS) functionality with a direct current voltage of 0 V vs. the open circuit potential and an alternating current voltage of 20 mV rms. The frequency range used was 60 kHz to 100 Hz, and values of R_{Ω} were determined using the first x-intercept of the Nyquist plot. Gamry's "Noise Reject" mode was used to improve the signal-to-noise ratio in SWVs.

Simulations were conducted using COMSOL Multiphysics® v5.6's Coefficient Form Partial Differential Equation interface. The mesh size was extremely fine and the time steps were six orders of magnitude below the assigned simulation run time.

5.2. Results and Discussion

We have previously shown^{5,9,54} that uncompensated Ohmic resistance can significantly attenuate electrochemical measurements. As such, to enable quantitative analysis of experimental data, SWVs were collected with varying amounts of positive-feedback IR $_{\Omega}$. As noted in Section 5.1, PEIS was used to determine the value of R $_{\Omega}$ as the first *x*-intercept of the generated Nyquist plot. A representative set of IR $_{\Omega}$ compensated voltammograms are shown in Fig. 16a below. Note the increase in the magnitude of the peak current and the sharpening of the voltammogram as the amount of positive-feedback IR $_{\Omega}$ increased. The half-width potential (W $_{1/2}$) measured for each of the voltammograms is shown in Fig. 16b. For a redox reaction involving a soluble-soluble transition, values of W $_{1/2}$ can be estimated through the following well-established equation:⁵⁷

$$W_{1/2} = 3.52 \frac{RT}{nF}$$
 [3]

Where R is the universal gas constant and T is the solution temperature. Note, in Fig. 16b, the measured half-width potential converged to values expected for a SWV corresponding to a two-electron transfer reaction conducted at 600° C (=132 mV).

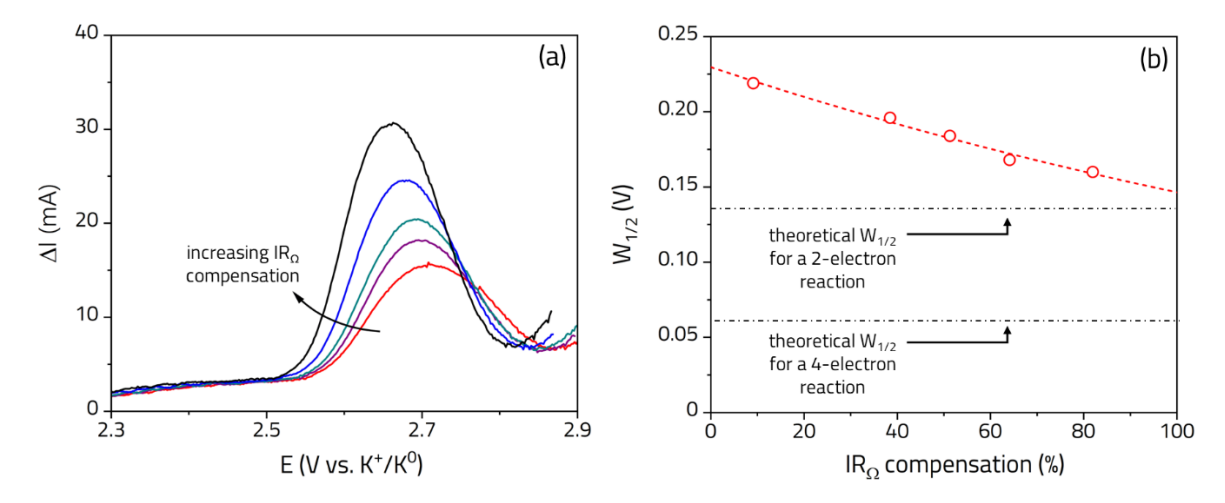


Figure 16. (a) Square wave voltammograms collected with various amounts of positive-feedback IR_{Ω} compensation, and (b) measured half-width potential as a function of IR_{Ω} compensation converging to values expected for a two-electron transfer reaction. The salt temperature was 600°C.

Measurements of electrochemical signatures corresponding to a two-electron transfer reaction have been routinely reported in a variety of molten salts. 58,59 However, in much of these studies, reaction mechanisms are largely attributed to the direct oxidation of oxides to gaseous oxygen according to the following redox reaction: $20^{2-} \rightarrow 0_2 + 4e$. In Fig. 16b, the expected value of $W_{1/2}$ associated with a four-electron reaction equals 66 mV, *i.e.*, a significantly lower value than empirical measurements. In these studies, fractional stoichiometric coefficients are then erroneously employed to reconcile the experimental data (wherein n=2) with the balanced reaction (wherein n=4). Furthermore, assignment of this reaction to oxygen evolution neglects fundamental electrochemical and physicochemical principles, as well as historical literature $^{60-62}$ that suggest the formation of soluble peroxide intermediates. In particular, gas evolution reactions are well-known to produce noisy electrochemical responses as a result of rapid and uncontrolled bubble effervescence; 63 signatures not observed in publications claiming to evolve oxygen gas.

Positive-feedback IR $_{\Omega}$ compensation provided a useful approach for academic interrogation of reaction mechanisms governing oxide speciation. However, its practical applicability to measurements conducted in industrial settings involving long cable lengths and noisy environments remains limited. As such, voltammograms were simulated to extract correction factors to post-experimentally correct IR $_{\Omega}$ -attenuated data. The detailed mathematical framework and assumptions underlying the construction of the simulations have been detailed elsewhere, ^{5,9,54} and for brevity are excluded from this report. In Fig. 17a, voltammograms simulated with varying amounts of IR $_{\Omega}$ contributions are depicted. Note, the depression in the magnitude of the peak difference current and dilation of the SWV as IR $_{\Omega}$ contributions increased. Current multipliers (CMs) were extracted from simulated voltammograms using the following relationship:

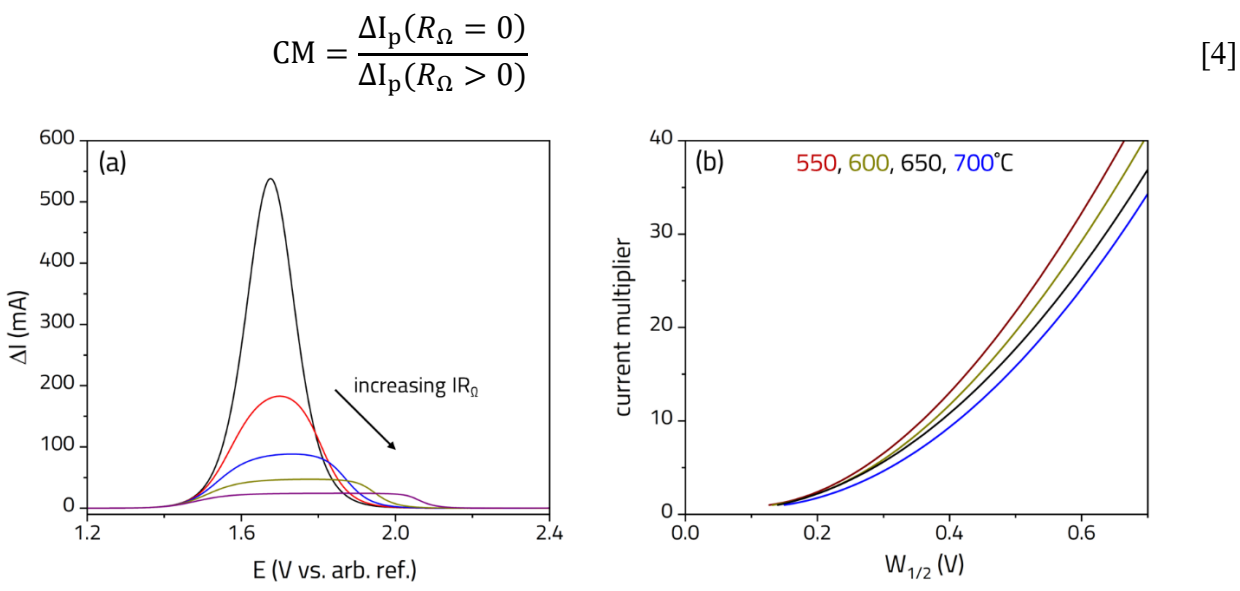


Figure 17. (a) Representative SWVs simulated with varying amounts of IR_{Ω} contributions, and (b) current multipliers as a function of the $W_{1/2}$ at various temperatures extracted from simulations

Fig. 17b shows the CM for a range of temperatures as a function of the half-width potential. Using these CMs, raw empirical data was corrected using:⁷

$$\Delta I_{p}^{corrected} = CM \times \Delta I_{p}^{uncorrected}$$
 [5]

Fig. 18a shows a representative set of experimental SWVs collected at 550°C. In Fig. 18b, a non-linear response was noted in the uncorrected peak difference current when plotted as a function of the square root of frequency. When the data was corrected using the CMs from Fig. 17b and Eq. 5, a linear relationship crossing through the origin was observed (as predicted by Eq. 1).

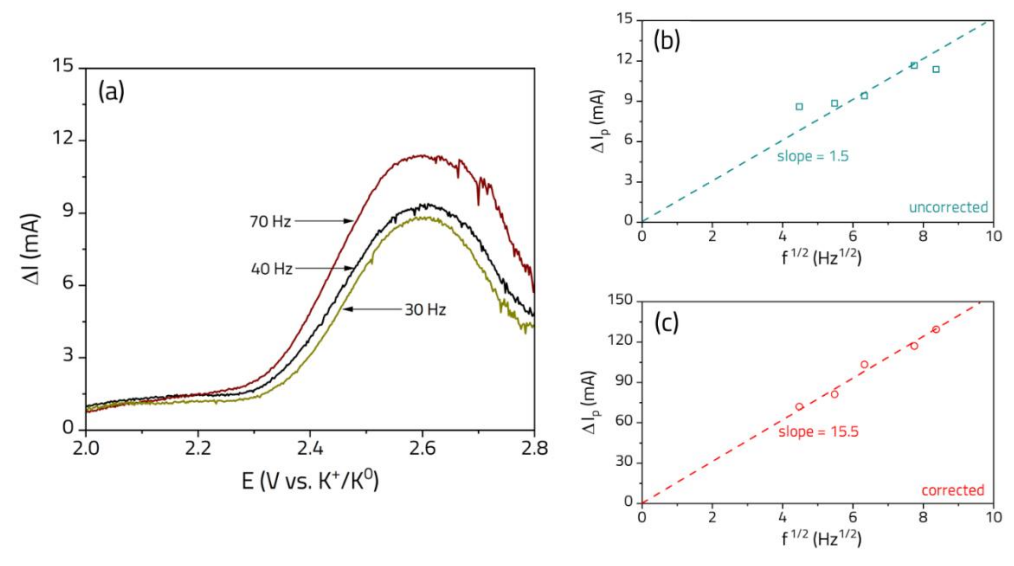


Figure 18. (a) Representative experimental SWVs collected at 30, 40, and 70 Hz, the (b) uncorrected and (c) corrected peak difference current versus the square root of frequency. The salt was 2.8 wt% Li₂O dissolved in molten FLiNaK maintained at a temperature of 550°C.

Data was further collected at various electrode immersion depths and operating temperatures to confirm Arrhenius relationships and calculate diffusion coefficients (according to Eq. 1) at relevant operating temperatures. Diffusion coefficients corrected using the CM approach and are shown in Fig. 19a. For comparison, uncorrected values were also included. Note, a linear Arrhenius curve was observed only when CMs were used. Neglecting to use the CM approach to account for non-negligible IR $_{\Omega}$ contributions consistently led to erroneous values, as was clearly evident by the non-linear relationship in Fig. 19b. The consequence of such erroneous determinations of D and neglect of uncompensated IR $_{\Omega}$ can be seen in the parity plot shown in Fig. 19b. Use of uncorrected data resulted in a premature estimate of solubility limits, as indicated by the plateau observed at 0.5 M, whereas the corrected yielded concentrations within 15% of the parity line. Underpredictions of solubility limits can lead to compounding concerns regarding the operational integrity of MSR systems.

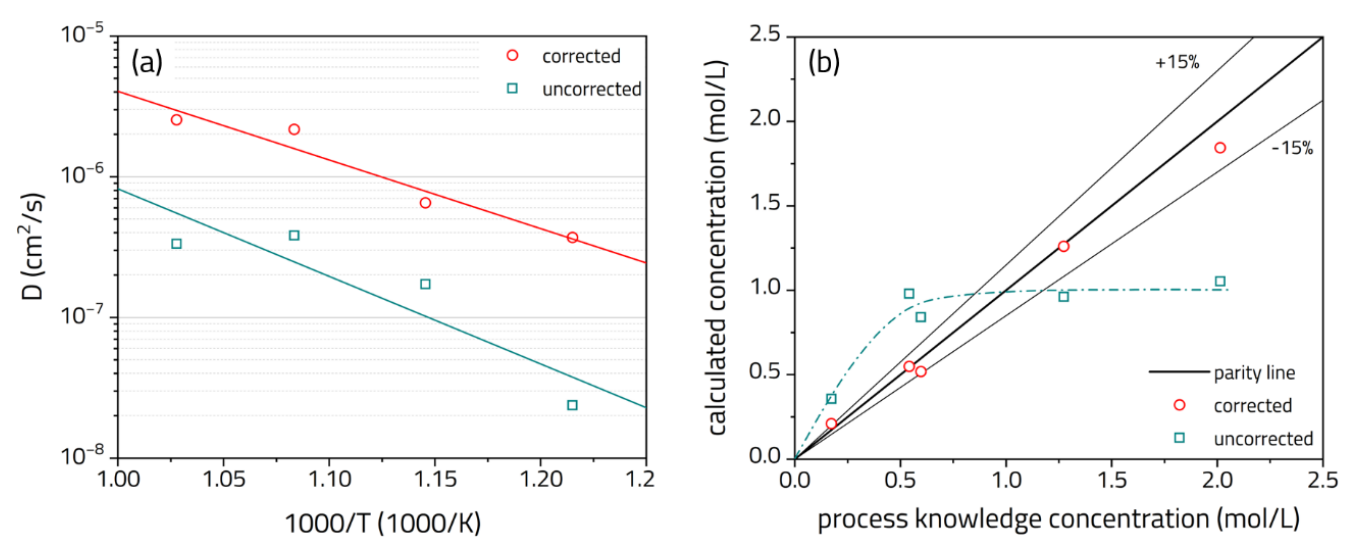


Figure 19. (a) Arrhenius and (b) parity plots corresponding to corrected (*red circles*) and uncorrected (*blue squares*) SWV data of the Li₂O-FLiNaK system. The parity plot was calculated using voltammetry data collected at 550°C.

6. Conclusions and Future Work

Efforts this year focused on the design, construction and installation of a pumped molten salt flow loop in a radiological glovebox. This loop was designed to enable modular testing of technologies under relevant MSR chemistries and flow conditions. The integration of the loop into a glovebox enables the safe handling of actinide-bearing molten salts while mitigating the risk of deleterious atmospheric ingressions. Performance testing of the pump was conducted using water prior to installation in the glovebox. Upgrades to the glovebox were also made in FY25 to prepare for operation of the pumped loops in FY26.

Fundamental electroanalytical studies were also conducted of reactive oxygen species in molten salts. Coupling numerical simulations with experimental activities, we developed capabilities to measure solution-phase reactive oxygen species in molten salts up to 10^{\times} higher loadings than what have been previously reported. Ultimately, these studies are necessary to enable targeted redox control and long-term operation of the molten salt testbeds in order to help technological development to progress at a rate beyond what was realized during the ARE- and MSRE-eras.

7. References

- 1. International Atomic Energy Agency, Technical Reports Series no. 489 Status of Molten Salt Reactor Technology, 2023.
- 2. International Atomic Energy Agency, IAEA Safeguards Glossary Edition, 2022.
- 3. Nuclear Regulatory Commission, 10CFR74 Material Control and Accounting of Special Nuclear Material.
- 4. N. C. Hoyt, *Fuel Salt Characterization and Qualification*, Molten Salt Fuel Cycle Chemistry Workshop, 2023.
- 5. N. A. Shaheen, J. Guo, and N. C. Hoyt, 2024, ANL/CFCT-24/28.
- 6. N. Hoyt, C. Pereira, J. Willit, and M. Williamson, FCRD-MPACT-2016-000401.
- 7. N. C. Hoyt, J. L. Willit, and M. A. Williamson, *J. Electrochem. Soc.*, 2017, 164(2), H134.
- 8. N. C. Hoyt, C. A. Launiere, and E. A. Stricker, *Nucl. Mater. Manag.*, 2021, 49(1), 87.
- 9. N. A. Shaheen and N. C. Hoyt, *J. Electrochem. Soc.*, 2025, 172, 086502.
- 10. H. C. Savage, E. Compere, J. M. Baker, and E. G. Bohlmann, 1967, ORNL-TM-1960.
- 11. J. L. Crowley, W. B. McDonald, and D. L. Clark, 1963, ORNL-TM-528.
- 12. D. B. Trauger and J. A. Conlin, Jr., Nucl. Sci. Eng., 1961, 9, 346.
- 13. R. C. Roberson, 1965, ORNL-TM-728.
- 14. W. D. Manly, G. M. Adamson, Jr., J. H. Coobs, J. H. DeVan, D. A. Douglas, E. E. Hoffman, P. Patriarca, 1957, ORNL-2349.
- 15. E. G. MacPherson, 1959, ORNL-2684.
- 16. W. B. McDonald and J. L. Crowley, 1960, ORNL-2688.
- 17. K. Robb, E. Kappes, and D. Orea, 2023, ORNL/LTR-2023/3087.
- 18. K. Robb and D. Orea, 2024, ORNL/LTR-2024/3671.
- 19. S. S. Raiman, et al., *J. Nucl. Mater.*, 2022, 561, 153551.
- 20. I. F. Saxena, B. Pint, and C. Lissenden, *Proceedings of Structural Health Monitoring*, 2023.
- 21. T. Hua, et al., *Digital Twins and Separate Effects Loop to Support Operation of a Stable Salt Reactor*, 2025, NURETH-21.
- 22. T. F. Fuerst, et al., Ann. Nucl. Energy, 2025, 223, 111659.
- 23. T. Fuerst, 2024, INL/MIS-24-77603.

- 24. K. M. Armijo, D. Dorsey, and A. Overacker, 2024, SAND2024-16619.
- 25. K. Britsch, M. Anderson, P. Brooks, and K. Sridharan, Int. J. Heat Mass. Transf., 2019, 134, 970.
- 26. Y. Wang, A. P. Olson, C. Falconer, B. Kelleher, I. Mitchell, H. Zhang, K. Sridharan, J. W. Engle, and A. Couet, *Nat. Commun.*, 2024, 15, 3106.
- 27. M. Zhang and J. Zhang, Lessons Learned from Operation of a Forced Convection Chloride Molten Salt Loop.
- 28. C. W. Forsberg, Flowing salt loop for the MIT reactor, TRISO fuel safeguards and irradiated graphite disposal, MSR Campaign Annual Review Meeting, 2025.
- 29. C. Forsberg, D. M. Carpenter, A. I. Hawari, R. O. Scarlat, and K. Robb, In-Pile Testing of Nuclear Fuels and Materials, 2020, 123(1), 475.
- 30. MSRR Abilene Christian University Application, U.S. NRC, link: www.nrc.gov/reactors/non-power/new-facility-licensing/msrr-acu.
- 31. Natura Resources, *Molten Salt Test System Operational*, 2024, link: https://www.naturaresources.com/molten-salt-test-system-operational.
- 32. Kairos Power, Kairos Power Logs 1,000 Hours of Pumped Salt Operations with its Non-Nuclear Engineering Test Unit, 2024, link: https://kairospower.com.
- W. Doniger, N. C. Hoyt, *In-line flow-enhanced electrochemical sensors for MSR mass accountancy*, Advanced Reactor Safeguards & Security Meeting, 2024.
- 34. Southern Company, Southern Company subsidiary and TerraPower complete installation of Integrated Effects Test, a key milestone in development of Molten Chloride Fast Reactor, link: https://www.southerncompany.com.
- 35. B. C. Kelleher, S. F. Gagnon, and I. G. Mitchell, *Mater. Today Commun.*, 2022, 33, 104358.
- 36. Copenhagen Atomics, Pumped Portable Molten Salt Loops, link: www.copenhagenatomics.com.
- 37. D. Zhang, L. Liu, M. Liu, R. Xu, C. Gong, Jun Zhang, C. Wang, S. Qiu, G. Su, *Int. J. Energy Res.*, 2018, 42(5), 1834.
- 38. *China refuels thorium reactor without shutdown*, Nuclear Engineering International, 2025, link: https://www.neimagazine.com/news/china-refuels-thorium-reactor-without-shutdown.
- 39. C. E. Moore, W. H. Doniger, and N. C. Hoyt, 2023, ANL/CFCT-23/28.
- 40. W. Doniger, M. Jubinsky, C. Moore, N. Shaheen, and N. Hoyt, 2024, ANL/CFCT-24/29.
- 41. C. E. Moore, W. H. Doniger, and N. C. Hoyt, 2022, ANL/CFCT-22/34.
- 42. D. Holcomb, *Module 7: Overview of MSR Instrumentation*, Presentation for U.S. Nuclear Regulatory Commission Staff, 2017.

- 43. S. Pantopoulou, A. Cilliers, L. Tsoukalas, and A. Heifetz, *Transfer Learning Long Short-Term Memory (TL-LSTM) Network for Molten Salt Reactor Sensor Monitoring*, ANS Winter Meeting, 2022.
- 44. J. Guo, C. Launiere, B. Cutrer, and N. Hoyt, 2022, ANL/CFCT-23/1.
- 45. J. McFarlane, D. Orea, K. Robb, B. Hunter, K. R. Johnson, H. Andrews, K. Lee, and R. Salko, 2024, ORNL/TM-2024/3579.
- 46. T. Carson, H. Kim, J. Se, and Y. Hassan, *Nucl. Eng. Des.*, 2025, 445, 114449.
- 47. Nuclear News, UM conducts molten salt experiment, NuclearNewswire, 2025, link: https://www.ans.org/news/2025-07-16/article-7194.
- 48. J. Guo, D. J. Johnson, A. Blockmon, and N. C. Hoyt, 2025, ANL/CFCT-25/13.
- 49. Vacuum Atmosphere Company, 2025, link: https://vacatm.com.
- 50. A. Polke, B. Cutrer, D. Penley, N. Shaheen, and N. Hoyt, *Molten Salt Reprocessing Sampler*, MPACT Technical Review Meeting, 2025.
- 51. H. W. Savage, W. F. Boudreau, E. J. Breeding, W. G. Cobb, W. B. McDonald, H. J. Metz, and E. Storto, Ch. 15, Equipment for molten-salt reactor heat-transfer systems.
- 52. L. Ramaley and M. S. Krause, Jr., *Anal. Chem.*, 1969, 41(11), 1363.
- 53. A. J. Bard and L. R. Faulkner, Electrochemical Methods Fundamentals and Applications (John Wiley & Sons, New York), 2001.
- 54. N. A. Shaheen, J. Guo, and N. C. Hoyt, *J. Electrochem. Soc.*, 2024, 171, 126502.
- 55. V. Mirčeski and M. Lovrić, J. Electroanal. Chem., 2001, 497, 114.
- 56. M. M. Tylka, J. L. Willit, J. Prakash, M. A. Williamson, J. Electrochem. Soc., 2015, 162, H625.
- 57. G. C. Barker, R. L. Faircloth, and A. W. Gardner, 1956, A.E.R.E. C/R 1786.
- 58. L. Massot, L. Cassayre, P. Chamelot, and P. Taxil, J. Electroanal. Chem., 2007, 606, 17.
- 59. M. Shen, H. Peng, M. Ge, Y. Zuo, and L. Xie, *J. Electroanal. Chem.*, 2015, 748, 24.
- 60. A. J. Appleby and S. Nicholson, J. Electroanal. Chem. Interf. Electrochem., 1974, 53, 105.
- 61. N. S. Wrench and D. Inman, J. Electroanal. Chem. Interf. Electrochem., 1968, 17, 319.
- 62. P. G. Zambonin and J. Jordan, *J. Am. Chem. Soc.*, 1969, 91, 9.
- 63. S. Abdelghani-Idrissi, N. Dubouis, A. Grimaud, P. Stevens, G. Toussaint, and A. Colin, *Sci. Rep.*, 2021, 11, 4677.
- 64. *Molten salt test loop at INL means real-time data on sensors and materials*, NuclearNewswire, 2025, link: https://www.ans.org/news/2025-04-03/article-6914/molten-salt-test-loop-at-inl-means-realtime-data-on-sensors-and-materials/

8. Appendix I

Survey of US-Based MSR-Relevant Flow Systems*									
Name	Facility/Laboratory	Salt type	Thermal or forced convection?	Flexibility/ Modularity	Actinide- bearing or FHR- relevant salt?	Size	Realistic flow conditions?	Scalable/ Capable of Mass Production?	References
Liquid Salt Test Loop (LSTL)	Oak Ridge National Laboratory	FLiNaK	Forced						[17]
Facility to Alleviate Salt Technology Risks (FASTR)		MgCl ₂ -NaCl-KCl	Forced						[17,18]
Thermal Convection Loops		FLiNaK, FLiBe, MgCl ₂ -NaCl- KCI	Thermal						[19,20]
Molten Salt Test Loop (MSTL)	Sandia National Laboratory	Nitrate salts for Solar Applications	Forced						[24]
Separate Effects Loop	Argonne National Laboratory	Chloride Salt	Forced						[21]
In-glovebox Actinide Salt Loops		Chloride Salt	Forced						This work
Modular Flow Instrumentation Testbed (MFIT)		Chloride Salt	Forced						[39-41]
NEXT Lab Molten Salt Test System	Abilene Christian University	FLiNaK	Forced						[31]
Molten Salt Research Reactor (MSRR)		FLiBe-U	Forced						[30,31]
INL Thermal Convection Loop	Idaho National Laboratory	Chloride Salt	Thermal						[64]
Molten Salt Tritium Transport Experiment (MSTTE)		FLiNaK	Forced						[22,23]
Engineering Test Unit (ETU)	Kairos Power	FLiBe	Forced						[32]
Salt Test Loops		FLiBe	Forced						[33]
Instrumentation Test Unit (ITU)		FLiNaK	Forced						[43]
Integrated Effects Test Loop	TerraPower	Chloride	Forced						[34]
Microloops		Chloride	Thermal						[35]
Shaft Seal Test Facility (SSTF)	University of Michigan	FLiNaK	Forced						[47]
Chloride Flow Loop	Virginia Tech	MgCl ₂ -NaCl-KCl	Forced						[27]
Liquid Salt Flow Loop	University of Wisconsin Madison	Nitrate, chloride, and fluoride salts	Forced						[26]
FliBe TCL		FLiBe	Thermal						[25]
Integrated Research Project (IRP) FLiBe Loop	Massachusetts Institute of Technology Collaboration with UC-Berkeley, NCSU, and ORNL	Fluoride salts	Forced						[28, 29]
Copenhagen Atomics Salt Loops	Loops deployed to various US institutions	Various fluoride salts	Forced						[36]

^{*}Based on publically available literature and sources



Chemical and Fuel Cycle Technologies Division

Argonne National Laboratory 9700 South Cass Avenue, Bldg. 205 Argonne, IL 60439

www.anl.gov

